Journal of Nuclear Medicine, published on January 25, 2018 as doi:10.2967/jnumed.117.205286

Patient-specific computational model and dosimetry calculations for a patient pregnant with twins undergoing a PET/CT examination

Tianwu Xie[1*], Paolo Zanotti-Fregonara[2], Agathe Edet-Sanson[3] and Habib Zaidi[1,4,5,6†]

[1]Division of Nuclear Medicine & Molecular Imaging, Geneva University Hospital, CH-1211 Geneva 4, Switzerland

[2]Houston Methodist Research Institute, Houston, TX, USA

[3]Department of Nuclear Medicine, Centre Henri Becquerel, Rouen, France

[4]Department of Nuclear Medicine and Molecular Imaging, University Medical Center 9700 RB Groningen, Groningen, Netherlands

[5]Geneva University Neurocenter, University of Geneva, 1205 Geneva, Switzerland

[6]Department of Nuclear Medicine, University of Southern Denmark, DK-500, Odense, Denmark

[†]**Corresponding author:**
Habib Zaidi, Ph.D
Geneva University Hospital
Division of Nuclear Medicine and Molecular Imaging
CH-1211 Geneva, Switzerland
Tel: +41 22 372 7258
Fax: +41 22 372 7169
email: habib.zaidi@hcuge.ch

[*]**First author:**
Tianwu Xie, Ph.D
Geneva University Hospital
Division of Nuclear Medicine and Molecular Imaging
CH-1211 Geneva, Switzerland
Fax: +41 22 372 7169
email: tianwuxie@gmail.com

Short running title: Fetal dosimetry in PET/CT

Figures: 7

Tables: 5

Abstract

Purpose: The radiation dose delivered to pregnant patients during radiological imaging procedures raises health concerns because the developing embryo and fetus are considered to be highly radiosensitive. To appropriately weigh the diagnostic benefits against the radiation risks, the radiologist needs reasonably accurate and detailed estimates of the fetal dose. Expanding our previously developed series of computational phantoms for pregnant women, we here describe a personalized model for twin pregnancy, based on an actual clinical scan.

Methods: The model is based on a standardized hybrid pregnant female and fetus phantom and on a clinical case of a patient who underwent an ^{18}F-fluoro-deoxyglucose (^{18}F-FDG) positron emission tomography (PET) / computed tomography (CT) scan while expecting twins at 25-weeks' gestation. This model enabled us to produce a realistic physical representation of the pregnant patient and to estimate the maternal and fetal organ doses from the ^{18}F-FDG and CT components. The N-Particle eXtended (MCNPX) general purpose Monte Carlo code was used for radiation transport simulation.

Results: The fetal ^{18}F-FDG doses for the two fetuses were 3.78 and 3.99 mGy, whereas the CT doses were 0.76 and 0.70 mGy, respectively. Therefore, the relative contribution of ^{18}F-FDG and CT to the total dose to the fetuses was about 84% and 16%, respectively. Meanwhile, for ^{18}F-FDG, the calculated personalized absorbed dose is about 40% - 50% higher than the values reported by other dosimetry computer software tools.

Conclusion: Our approach for constructing personalized computational models allows the estimation of patient-specific radiation dose, even in cases with unusual anatomical features, such as a twin pregnancy. Our results also show that, even in twins, the fetal organ doses from both ^{18}F-FDG and CT present a certain variability linked to the anatomic characteristics. The CT fetal dose is smaller than the ^{18}F-FDG PET dose.

Key words: CT, radiation dosimetry, fetus, pregnant female models, Monte Carlo simulation.

Key points:

- The dose calculated using patient-specific models may significantly differ from that calculated using standard anthropomorphic phantoms.
- The absorbed dose is non-uniformly distributed between the two fetuses.
- This work reports, for the first time, estimates of fetal organ-level dose for twins.
- The absorbed dose of fetal brain and skeleton is higher than other fetal tissues.
- The developed methodology is adequate for patient-specific radiation dosimetry.

Pregnant females are critical patients in whom the benefit from radiological examinations must be carefully weighed against the possible radiation risk to the fetus. At fetal doses greater than 50-100 mGy, which are unlikely to be delivered by medical imaging, the potential hazard effects of radiation on the fetus include embryonic death, intra-uterine growth limitation, average intelligence quotient loss, mental retardation, organ malformation, and small head size (*1*). Although controversial (*2*,*3*), the linear no-threshold model still provides the basis of radioprotection regulations. This model postulates that stochastic effects, such as cancer, might also occur at smaller doses (*4*-*8*). Because of this regulatory framework, and because health effects cannot be formally ruled out, the fetal absorbed doses should be known as precisely as possible. Estimating the fetal dose is however a challenging task, owing to the difficulties associated with direct measurement of energy deposition and the irregular shape of the fetal body. Different approaches have been adopted to estimate the fetal dose, including Monte Carlo simulations using computational anthropomorphic models (*7*,*9*-*17*) and experimental measurements using physical phantoms with embedded dosimeters (*18*-*21*). However, these approaches inherently bear a number of limitations, such as the difficulty of constructing patient-specific computational models and the difficulty of matching anthropomorphic physical phantoms to the size and location of the fetus within the maternal body (*22*). Because of these limitations, significant over- or under-estimations of the fetal absorbed dose are possible. Monte Carlo calculations are considered the gold standard for dose estimation in diagnostic imaging (*23*), and their use in a clinical setting within a framework of patient-specific estimation of fetal dose from diagnostic examination procedures is highly desirable.

In this work, we expand on our previous set of anthropomorphic phantoms and describe the methodology for constructing patient-specific computational models for a pregnant female with twins. This model is based on a standardized hybrid pregnant-female-and-fetus phantom, derived from an actual 25-weeks' pregnant patient who underwent an ^{18}F-fluoro-deoxyglucose (^{18}F-FDG) positron emission tomography/computed tomography (PET/CT) scan while expecting twins. The patient-specific maternal and fetal absorbed radiation doses from both ^{18}F-FDG and CT were calculated and compared with the results provided by the OLINDA/EXM software (*24*) and ImPACT CT (Impact Performance Assessment of CT, Bence Jones Offices, St. George's Hospital, London) dosimetry calculator, respectively. The influence of fetal position on fetal absorbed dose was also investigated.

MATERIALS AND METHODS

Standardized Computational Model For Twins

A standardized pregnant female model with twins at 25th weeks of gestation was developed based on the International Commission on Radiological Protection (ICRP) computational pregnant female phantom at 25th weeks of gestation (*17*) developed using the mother torso and internal organs of the Rensselaer Polytechnic Institute phantoms (RPI-P) (*25*), the Fetal and Mother Numerical Models of Telecom ParisTech (*26*), the Katja model (*27*) and the newborn model of Helmholtz Zentrum München (*28*). The 25th-week twins phantom was developed based on the fetal and mother numerical models and the Katja model. The organs of the fetus were scaled from the Katja model to match the reference organ masses of the ICRP (*29*). The maternal bladder, small intestine (SI) and large intestine (LI) were manually adjusted using the Rhinoceros™ package. A total of 35 maternal tissues (including adrenals, urinary bladder (UB) wall, urinary bladder (UB) content, brain, breasts, esophagus, eyeballs, eye lenses, gallbladder wall, gallbladder content, heart wall, heart content, kidneys, LI wall, LI content, liver, lungs, ovaries, pancreas, small intestine, skeleton, skin, spleen, stomach wall, stomach content, thymus, thyroid, trachea, uterine wall, uterine content, placenta, umbilical cord, amniotic fluid, yolk sac, and remainder tissues) and 50 fetal regions (25 for each fetus) were included in our model. The fetal tissue compositions were obtained from the ICRP 89 (*29*): the bone density was set at 1.3g/cm^3 and the soft-tissue density at 0.99g/cm^3.

Patient-specific Computational Model

The CT images of the pregnant patient were segmented into body, lung, skeleton and uterus for constructing the regional voxel matrix (Fig. 1). This retrospective study reported in previous work (*30*) didn't require additional institutional review board approval and the requirement to obtain informed consent was waived. Firstly, the standardized twins computational model was voxelized from the boundary representation model and then registered using the Insight Toolkit (*31*) to the constructed CT-derived regional patient-specific voxel matrix using automatic affine registration to produce a new personalized computational model with well-defined anatomical structures, matching CT patient images. The developed patient-specific computational model was used as input for Monte Carlo calculations of the radiation dose to the fetus and maternal body. Fig. 2 shows the 3D visualization of the constructed patient-specific model with zoomed-in views of the upper fetus and lower fetus. Fig. 3 shows the

registration of representative CT images between the patient and the standardized computational phantom for the construction of the patient-specific model.

Monte Carlo Simulations

PET component

The patient-specific computational phantom was imported to the The N-Particle eXtended (MCNPX) code (*32*) for radiation transport simulations. S-values of uniformly distributed sources of ^{18}F in maternal and fetal tissues were estimated. The absorbed dose and effective dose delivered to both fetuses and maternal organs from ^{18}F-FDG were calculated based on the Medical Internal Radiation Dose formalism (*33*). The regions of interest used for calculating the activity concentrations in the fetuses were manually drawn on the body of the fetuses (*30*). The time-integrated activity coefficients of ^{18}F-FDG in maternal organs was obtained from ICRP publication 106 (*34*). Table 1 lists the total number of disintegrations (residence times) of ^{18}F-FDG in maternal organs and the two fetuses. An equal average activity concentration in fetal tissues for each fetus was assumed. The mean total number of disintegrations of ^{18}F-FDG in the upper fetus and lower fetus are 0.0412 and 0.0434 Bq h/Bq, respectively.

CT component

A GE 750HD CT scanner model has been created and validated using Monte Carlo-based techniques in our previous works (*12*,*35*). This CT source and geometry model is equipped with Performix Pro VCT 100 x-ray tube with 56 degree fan-beam angle, 7 degree target angle and measured half-value layer of 7.8 mm Al at 120 kVp. The patient-specific computational model was integrated with the CT scanner model in the N-Particle eXtended code (*32*). Simulated CT examinations were performed using the personalized model and the protocol parameters used in our institution for patients scanning with a helical source path and total collimation width of 64×0.625 mm (*12*). The absorbed dose to maternal organs and fetal organs were calculated and normalized to the CT dose index ($CTDI_{vol}$ = 1.8 mGy) of the simulated examination (*12*).

Absorbed Dose Calculations

For the PET component, the radiation absorbed dose from ^{18}F-FDG to the target tissue r_T is given by:

$$\mathrm{D}(r_T, T_D) = \sum_{r_S} A(r_T, T_D)\, S(r_T \leftarrow r_S) \quad , \tag{1}$$

where r_S is the source organ, $A(r_T, T_D)$ is the cumulated activity in the source organ over the dose-integration period T_D, $S(r_T \leftarrow r_S)$ is the S-value describing the equivalent dose rate in the target organ per unit activity in the source organ.

For the CT component, the $CTDI_{vol}$-normalized radiation absorbed dose from the simulated to the clinical examination is estimated using the following equation:

$$\frac{D_{r_T}^{patient}}{CTDI_{vol}^{patient}} = \frac{D_{r_T}^{sim}}{CTDI_{vol}^{sim}} \quad , \tag{2}$$

where $CTDI_{vol}^{sim}$ is the $CTDI_{vol}$ of the patient in the simulated CT scanner, $D_{r_T}^{sim}$ is the calculated absorbed dose to the patient in the simulated CT scanner, $D_{r_T}^{patient}$ and $CTDI_{vol}^{patient}$ are the absorbed dose and $CTDI_{vol}$ to the patient in the clinical CT examinations, respectively. The reported $CTDI_{vol}$ for the patient in the clinical CT examination is 1.04 mGy. For the same patient model, the coefficient of variation for the $CTDI_{vol}$-normalized dose values across different scanners and protocols has been reported to be less than 10% (*36*).

RESULTS

Patient-specific Computational Phantom

The accuracy of the registration between the regional voxel matrix of the patient and the generated patient-specific computational phantom was evaluated by calculating Jaccard's coefficient of similarity (*37*) for the corresponding segmented organs. The Jaccard's coefficient of similarity for the total body, lung, skeleton and uterus are 0.73, 0.60, 0.12 and 0.55, respectively. The low Jaccard's coefficient for the skeleton is mainly caused by the mismatch of the ribs and hip bones between the anchor phantom and patient. The weight of the lower fetus matched well the ICRP-recommended fetal weight of 990g at 25-weeks' gestation, whereas the weight of the upper fetus was slightly lower (Table 2).

Absorbed Doses From The PET Component

The coefficient of variation of ^{18}F-FDG organ dose between the two fetuses was approximately 8.5%, with a minimum of approximately 0.3% (for spinal cord) and a maximum of approximately 23.2% (for the eyes) while the mean differences of the fetal total body dose between this work and the two versions of OLINDA/EXM are -55% and -40.5% (Table 3). As shown in Fig. 4A, for the same organ, the estimated self-absorbed S-value of the lower

fetus is about 29% smaller than the values of the upper fetus. Indeed, the self-absorbed S-values of fetal organs decrease when the fetal weight increases (*17*). The cross-absorbed S-values were obtained assuming uniform activity in all maternal source tissues. As shown in Figs. 4B and 4C, the cross-absorbed S-values for the maternal body irradiating the fetus are mostly contributed by the annihilation photons and present a uniform distribution in different fetal organs. The mean absolute difference of cross-absorbed S-values from the maternal body between the two fetuses is about 8%. The cross-absorbed S-values from maternal UB are affected by the fetal position and present a mean absolute difference of 112% between the two fetuses. Fig. 5 illustrates the organ absorbed dose in the two fetuses from ^{18}F-FDG. In the upper fetus, the gastrointestinal tract receives the highest absorbed dose while in the lower fetus the absorbed dose to the eyes and bone marrow is higher than in the other organs. The ^{18}F-FDG absorbed doses for the upper fetus and lower fetus are 0.0201 mGy/MBq and 0.0212 mGy/MBq, respectively. The absorbed dose for the maternal uterus is 11.4% and 16.2% lower than the total body dose of the upper fetus and the lower fetus, respectively.

Absorbed Doses From The CT Component

Except for the fetal total body, the fetal skeleton and bone marrow, the CT absorbed doses to other fetal organs are about 20% lower than the dose to the maternal uterus. The variation of CT organ dose between the two fetuses is approximately 5.7%, with a minimum of approximately 0.3% (for the liver) and a maximum of approximately 15.2% (for the brain). Fig. 6 compares the $CTDI_{vol}$-normalized absorbed dose for different maternal organs with estimates provided by the ImPACT CT dosimetry calculator. The mean absolute dose difference to the maternal organs between this work and ImPACT CT is 40.3%. Fig. 7 shows the $CTDI_{vol}$-normalized absorbed dose from the CT component to fetal organs. The absorbed dose is non-uniformly distributed between fetal organs. For instance, the absorbed dose to the fetal skeleton and bone marrow is about 3.7 and 2.0 times higher, respectively, than that received by other fetal organs. Since a low-dose CT scan protocol was performed, the absorbed doses to the two fetuses are relatively low, 0.73 mGy/$CTDI_{vol}$ and 0.67 mGy/$CTDI_{vol}$, respectively, while the absorbed dose to the uterus is 0.61 mGy/$CTDI_{vol}$.

Total Absorbed Doses From The Combined PET/CT Examination

The absorbed dose to the upper fetus is 0.76 mGy from the CT component and 3.78 mGy from the PET component, for a total of 4.53 mGy from the PET/CT examination while the absorbed dose to the lower fetus is 0.70 mGy from the CT component and 3.99 mGy from the PET component, for a total of 4.69 mGy from the PET/CT examination. In this study, for different fetal organs, the CT component contributes 8.4% - 30.8% of the total absorbed dose whereas the PET component contributes 70% - 91.6% of the total absorbed dose. For this patient, the ^{18}F-FDG activity injected to the patient is 188 MBq whereas the patient-specific $CTDI_{vol}$ performed in the CT examination is 1.04 mGy without tube current modulation. The calculated absolute doses to the patient and fetuses are summarized in Tables 4 and 5, respectively. The patient's effective dose is 0.79 mSv from the CT component and 3.62 mSv from the PET component resulting in a total of 4.41 mSv from the PET/CT examination.

DISCUSSION

We described the methodological procedure followed to create a computational patient-specific phantom enabling the calculation of the fetal dose in the particular case of twin pregnancy. Our approach, which involves the coregistration of clinical images to the computational phantom, followed by Monte Carlo-based dose calculations, is suitable for adoption in a clinical setting for individualized dose assessment. The unusual anatomy of a twin pregnancy is a clear example of the adaptability of our methodology to disparate clinical situations.

For the calculation of the fetal dose, there are three main sources of inaccuracy: 1) from the geometrical point of view, the registration of the standardized phantom to the clinical images, 2) the uncertainty linked to Monte Carlo simulations and 3) the $CTDI_{vol}$-based dose estimation to the organs. The uncertainty from the image registration process is by far the highest one, accounting for 27% - 45% of the variability in the dose, whereas the error expected from Monte Carlo calculations and $CTDI_{vol}$-based organ dose estimation is generally less than 5%. The $CTDI_{vol}$ and the dose length product are the two metrics commonly conveyed in dose reports by commercial CT scanners and used to report CT doses to pregnant patients and fetus (*12*).

The estimation of the CT dose shows that the fetal skeleton and bone marrow receive a substantially higher dose than soft tissues owing to their higher density. Although never proven for the range of doses received during medical examinations, radiation exposure of the bone marrow in childhood exposes the fetus to the hypothetical

risk of developing malignancies later in life, and this aspect should be taken into account when designing the acquisition protocol for the CT component.

The influence of anatomical characteristics of the fetus on radiation dosimetry was investigated by comparing the organ dose of the two fetuses. For the PET component, the coefficient of variation across the two fetuses for a given organ ranged from 0.3% (for the spinal cord) to 23.2% (for the eyes) with a mean across all organs of 8.5%. For the CT component, the coefficient of variation across the two fetuses for a given organ ranged from 0.3% (for liver) to 15.2% (for the brain) with a mean across all organs of 5.7%. These results indicate that, at the same gestation, the anatomical differences between the fetuses influence the estimation of the internal and external absorbed doses for any organ. The fetal organ dose to a particular fetus would be within approximately 25% of the mean value across the whole fetus at the same gestation. From a radiobiological point of view, this difference of absorbed dose between the two fetuses is likely to be non-significant.

An important finding of our study it that the fetal doses estimated using either OLINDA/EXM 1.1 or 2.0 are about 50% smaller than the values calculated using our patient-specific model. This discrepancy can be mainly attributed to the differences between fetus weights and source-fetus distances between the personalized computational phantom adopted in this work and patient's images and those used in OLINDA/EXM 1.1 and 2.0, which use a stylized model (*38*) and the 6-months voxel-based RPI-P model (*25*), respectively. When generic anthropomorphic phantoms, such as those included in both versions of OLINDA/EXM, are used, the final dose is heavily dependent on the characteristics of the phantom, such as the mass and the geometric arrangement of the organs. The use of a patient-specific phantom in a clinical setting allows more accurate dose calculation, which is of particular importance in cases like pregnant women or pre-therapeutic imaging. In radiation dosimetry, the absorbed dose to the maternal uterus is used as a conservative proxy for the fetal dose (*39*). This work shows that the mean fetal dose is about 15% higher than the uterus dose, for both PET and CT components. For CT, the uterus dose may still be used as a conservative value for fetal soft tissues (i.e. except for the skeleton and bone marrow).

Our study showed that the ^{18}F-FDG contribution to the total dose is much higher than the CT contribution, for both the mother and the fetuses (i.e. about 16-18% vs 82-84%). In addition, the maximum contribution to the organ dose from CT is about 30% to the fetal skeleton, whereas the maximum contribution from ^{18}F-FDG is over 90% to the brain, eyes and salivary gland. In total, the mean fetal dose from the PET/CT examination is 4.61 mGy. This

level of radiation is not only well below the threshold of deterministic effects, but is also below the threshold where stochastic effects have been documented in humans (*40*). When imaging pregnant women, the priority should be given to achieving an examination of diagnostic quality, as aggressive dose reduction protocols tend to overweigh the radiation risk and may put the life of both the mother and the fetus in danger (*41*).

CONCLUSION

The proposed approach for constructing personalized computational models enables the calculations of patient-specific radiation dose during combined PET/CT examination, even in complex unusual situations, such as a patient pregnant with twins. The fetal organ dose is particularly affected by the fetal position among other factors. The calculated personalized ^{18}F-FDG fetal dose is significantly higher than the corresponding CT dose and is about 40% - 50% higher than values reported by widely used popular internal dosimetry software.

ACKNOWLEDGMENTS

This work was supported by the Swiss National Science Foundation under Grant SNSF 320030_176052. The authors would like to thank Drs X. George Xu (Rensselaer Polytechnic Institute), Isabelle Bloch (Telecom ParisTech) and Maria Zankl (Helmholtz Zentrum München) for providing the computational models.

References

1. McCollough CH, Schueler BA, Atwell TD, et al. Radiation exposure and pregnancy: when should we be concerned? *Radiographics.* 2007;27:909-917; discussion 917-908.

2. Siegel JA, Sacks B. Eliminating use of the linear no-threshold assumption in medical imaging. *J Nucl Med.* 2017;58:1014-1015.

3. Tirada N, Dreizin D, Khati NJ, Akin EA, Zeman RK. Imaging pregnant and lactating patients. *Radiographics.* 2015;35:1751-1765.

4. ICRP. Publication 84: Pregnancy and medical radiation. *Ann ICRP.* 2000;30:iii-viii, 1-43.

5. ICRP. Publication 90: Biological effects after prenatal irradiation (embryo and fetus). *Ann ICRP.* 2003;33:5-206.

6. Pearce MS, Salotti JA, Little MP, et al. Radiation exposure from CT scans in childhood and subsequent risk of leukaemia and brain tumours: a retrospective cohort study. *Lancet.* 2012;380:499-505.

7. Helmrot E, Pettersson H, Sandborg M, Alten JN. Estimation of dose to the unborn child at diagnostic X-ray examinations based on data registered in RIS/PACS. *Eur Radiol.* 2007;17:205-209.

8. American College of Radiology. ACR-SPR Practice Parameter for Imaging Pregnant or Potentially Pregnant Adolescents and Women with Ionizing Radiation. Revised 2013 (Resolution 48), Reston (VA). 2013.

9. Angel E, Wellnitz CV, Goodsitt MM, et al. Radiation dose to the fetus for pregnant patients undergoing multidetector CT imaging: Monte Carlo simulations estimating fetal dose for a range of gestational age and patient size. *Radiology.* 2008;249:220-227.

10. Damilakis J, Perisinakis K, Tzedakis A, Papadakis AE, Karantanas A. Radiation dose to the conceptus from multidetector CT during early gestation: a method that allows for variations in maternal body size and conceptus position. *Radiology.* 2010;257:483-489.

11. Damilakis J, Tzedakis A, Perisinakis K, Papadakis AE. A method of estimating conceptus doses resulting from multidetector CT examinations during all stages of gestation. *Med Phys.* 2010;37:6411-6420.

12. Xie T, Poletti PA, Platon A, Becker CD, Zaidi H. Assessment of CT dose to the fetus and pregnant female patient using patient-specific computational models. *Eur Radiol.* 2018 doi: 10.1007/s00330-017-5000-z. [Epub ahead of print]

13. Gu J, Xu XG, Caracappa PF, Liu B. Fetal doses to pregnant patients from CT with tube current modulation calculated using Monte Carlo simulations and realistic phantoms. *Radiat Prot Dosimetry.* 2013;155:64-72.

14. Lopez-Rendon X, Walgraeve MS, Woussen S, et al. Comparing different methods for estimating radiation dose to the conceptus. *Eur Radiol.* 2017;27:851-858.

15. Maynard MR, Long NS, Moawad NS, et al. The UF Family of hybrid phantoms of the pregnant female for computational radiation dosimetry. *Phys Med Biol.* 2014;59:4325-4343.

16. Winer-Muram HT, Boone JM, Brown HL, Jennings SG, Mabie WC, Lombardo GT. Pulmonary embolism in pregnant patients: fetal radiation dose with helical CT. *Radiology.* 2002;224:487-492.

17. Xie T, Zaidi H. Development of computational pregnant female and fetus models and assessment of radiation dose from positron-emitting tracers. *Eur J Nucl Med Mol Imaging.* 2016;43:2290–2300.

18. Chatterson LC, Leswick DA, Fladeland DA, Hunt MM, Webster S, Lim H. Fetal shielding combined with state of the art CT dose reduction strategies during maternal chest CT. *Eur J Radiol.* 2014;83:1199-1204.

19. Jaffe TA, Neville AM, Anderson-Evans C, et al. Early first trimester fetal dose estimation method in a multivendor study of 16- and 64-MDCT scanners and low-dose imaging protocols. *AJR Am J Roentgenol.* 2009;193:1019-1024.

20. Kelaranta A, Kaasalainen T, Seuri R, Toroi P, Kortesniemi M. Fetal radiation dose in computed tomography. *Radiat Prot Dosimetry.* 2015;165:226-230.

21. Solomou G, Papadakis AE, Damilakis J. Abdominal CT during pregnancy: a phantom study on the effect of patient centring on conceptus radiation dose and image quality. *Eur Radiol.* 2015;25:911-921.

22. Zaidi H, Xu XG. Computational anthropomorphic models of the human anatomy: the path to realistic Monte Carlo modeling in medical imaging. *Annu Rev Biomed Eng.* 2007;9:471-500.

23. Zaidi H, Ay M. Current status and new horizons in Monte Carlo simulation of X-ray CT scanners. *Med Biol Eng Comput.* 2007;45:809-817.

24. Stabin MG, Sparks RB, Crowe E. OLINDA/EXM: The second-generation personal computer software for internal dose assessment in nuclear medicine. *J Nucl Med.* 2005;46:1023-1027.

25. Xu XG, Taranenko V, Zhang J, Shi C. A boundary-representation method for designing whole-body radiation dosimetry models: pregnant females at the ends of three gestational periods—RPI-P3, -P6 and -P9. *Phys Med Biol.* 2007;52:7023-7044.

26. Bibin L, Anquez J, de la Plata Alcalde JP, Boubekeur T, Angelini ED, Bloch I. Whole-body pregnant woman modeling by digital geometry processing with detailed uterofetal unit based on medical images. *IEEE Trans Biomed Eng.* 2010;57:2346-2358.

27. Becker J, Zankl M, Fill U, Hoeschen C. Katja — the 24th week of virtual pregnancy for dosimetric calculations. *Pol J Med*

Phys Eng. 2008;14:13-20.

28. Petoussi-Henss N, Zankl M, Fill U, Regulla D. The GSF family of voxel phantoms. *Phys Med Biol.* 2002;47:89-106.

29. ICRP. Publication 89: Basic anatomical and physiological data for use in radiological protection: reference values. *Annals of the ICRP.* 2002;32:1-277.

30. Zanotti-Fregonara P, Chastan M, Edet-Sanson A, et al. New fetal dose estimates from 18F-FDG administered during pregnancy: Standardization of dose calculations and estimations with voxel-based anthropomorphic phantoms. *J Nucl Med.* 2016;57:1760-1763.

31. Johnson HJ, McCormick MM, Ibanez L, and the Insight Software Consortium. The ITK software guide.; 2005.

32. Pelowitz DB. *MCNPX User's Manual Version 2.5.0.* Los Alamos, NM: Los Alamos National Laboratory; 2005. LA-CP-05-0369.

33. Bolch WE, Eckerman KF, Sgouros G, Thomas SR. MIRD Pamphlet No. 21: A generalized schema for radiopharmaceutical dosimetry - Standardization of nomenclature. *J Nucl Med.* 2009;50:477-484.

34. ICRP. publication 106: Radiation dose to patients from radiopharmaceuticals. Addendum 3 to ICRP Publication 53. *Ann ICRP.* 2008;38:1-197.

35. Akbarzadeh A, Ay MR, Ghadiri H, Sarkar S, Zaidi H. Measurement of scattered radiation in a volumetric 64-slice CT scanner using three experimental techniques. *Phys Med Biol.* 2010;55:2269-2280.

36. Turner AC, Zankl M, DeMarco JJ, et al. The feasibility of a scanner-independent technique to estimate organ dose from MDCT scans: using CTDIvol to account for differences between scanners. *Med Phys.* 2010;37:1816-1825.

37. Jackson DA, Somers KM, Harvey HH. Similarity coefficients: Measures of co-occurrence and association or simply measures of occurrence? *Am Nat.* 1989;133:436-453.

38. Stabin M, Watson E, Cristy M, et al. *Mathematical models and specific absorbed fractions of photon energy in the nonpregnant adult female and at the end of each trimester of pregnancy*: Oak Ridge National Lab., TN (United States); Report ORNL/TM-12907, 140 p, 1995.

39. Petoussi-Henss N, Schlattl H, Zankl M, Endo A, Saito K. Organ doses from environmental exposures calculated using voxel phantoms of adults and children. *Phys Med Biol.* 2012;57:5679-5713.

40. Brent RL. Protection of the gametes embryo/fetus from prenatal radiation exposure. *Health Phys.* 2015;108:242-274.

41. Zanotti-Fregonara P, Hindie E. Performing nuclear medicine examinations in pregnant women. *Phys Med.*

2017;43:159-164.

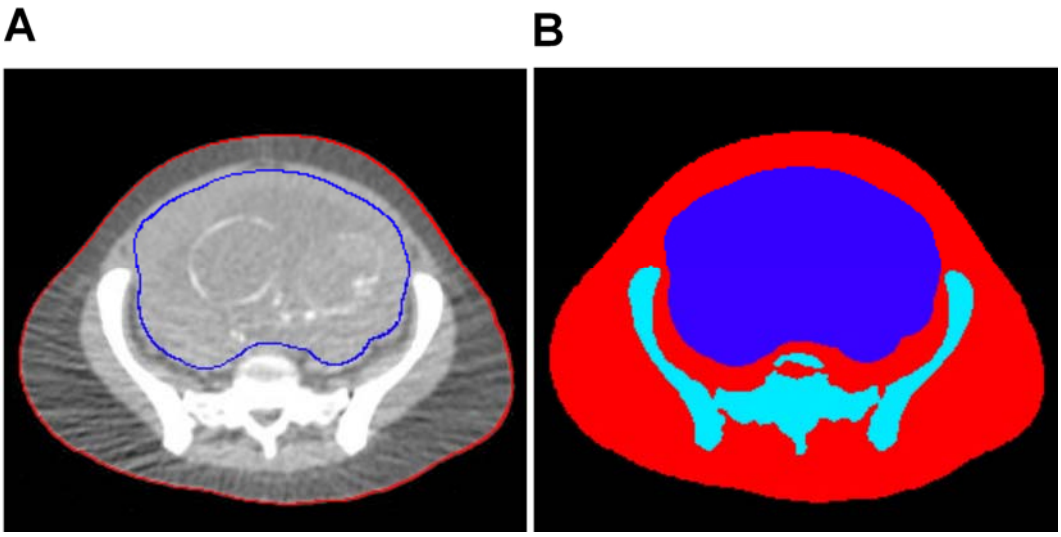

Fig. 1. (A) CT image with external body contour (red line) around the perimeter of the pregnant patient and the uterus (blue line) containing 25-week-old twin fetuses. (B) Segmented CT image with external body contour, skeleton and uterus.

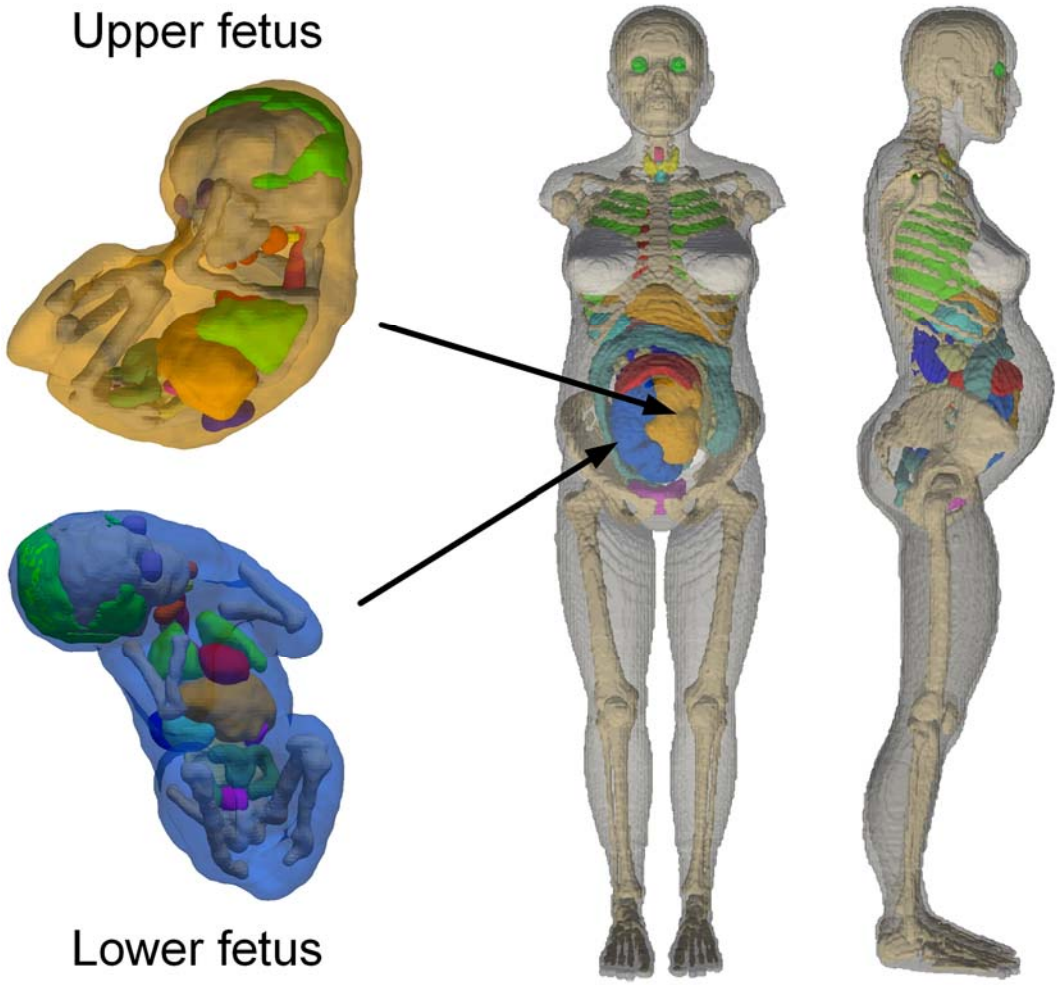

Fig. 2. 3D views of the computational pregnant female phantom at 25 weeks gestation age with zoomed views of the embedded twins.

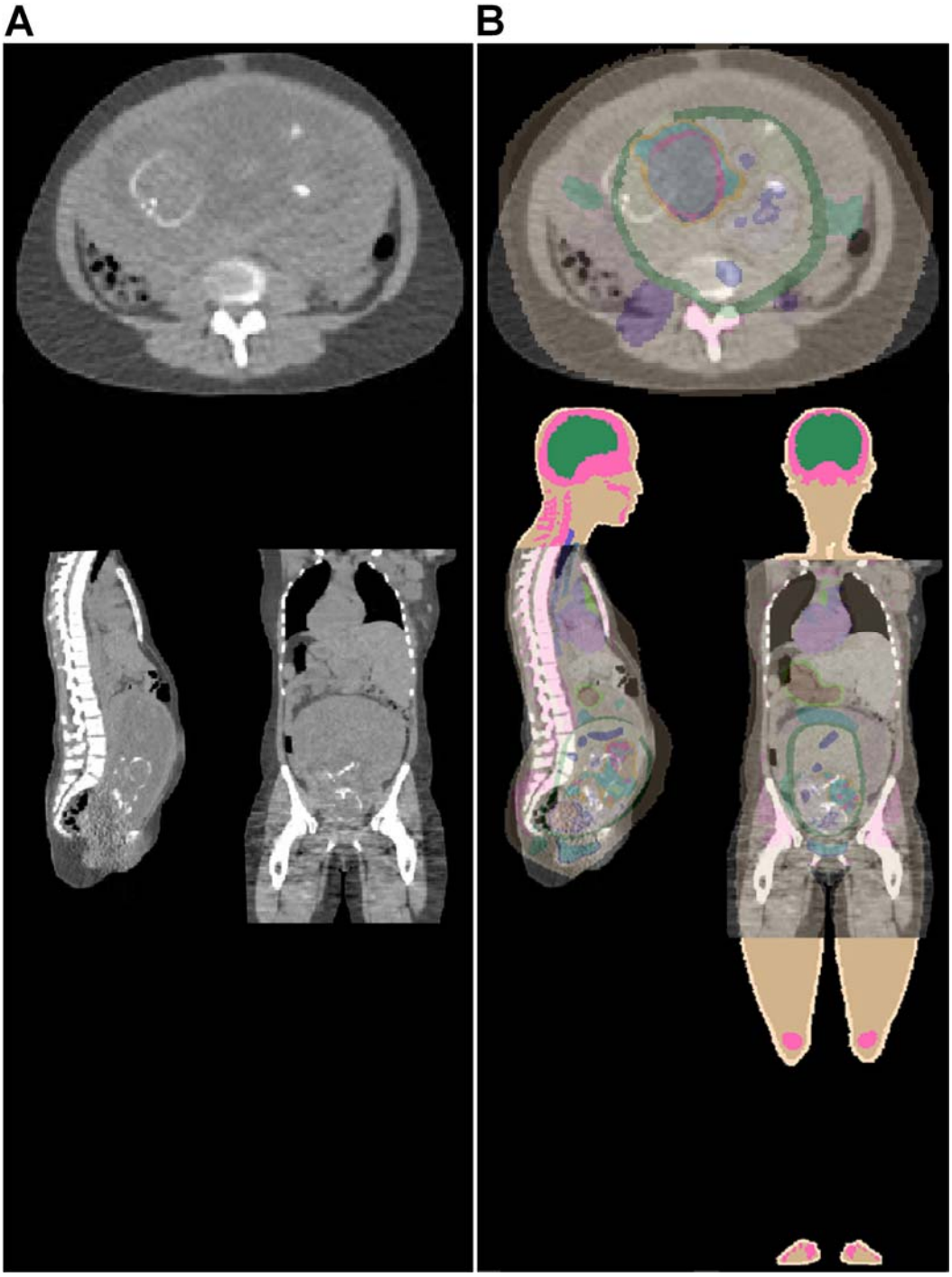

Fig. 3. Representative slices showing image registration between (A) abdominal CT images of the patient and (B) the computational phantom for the development of patient-specific pregnant computational models.

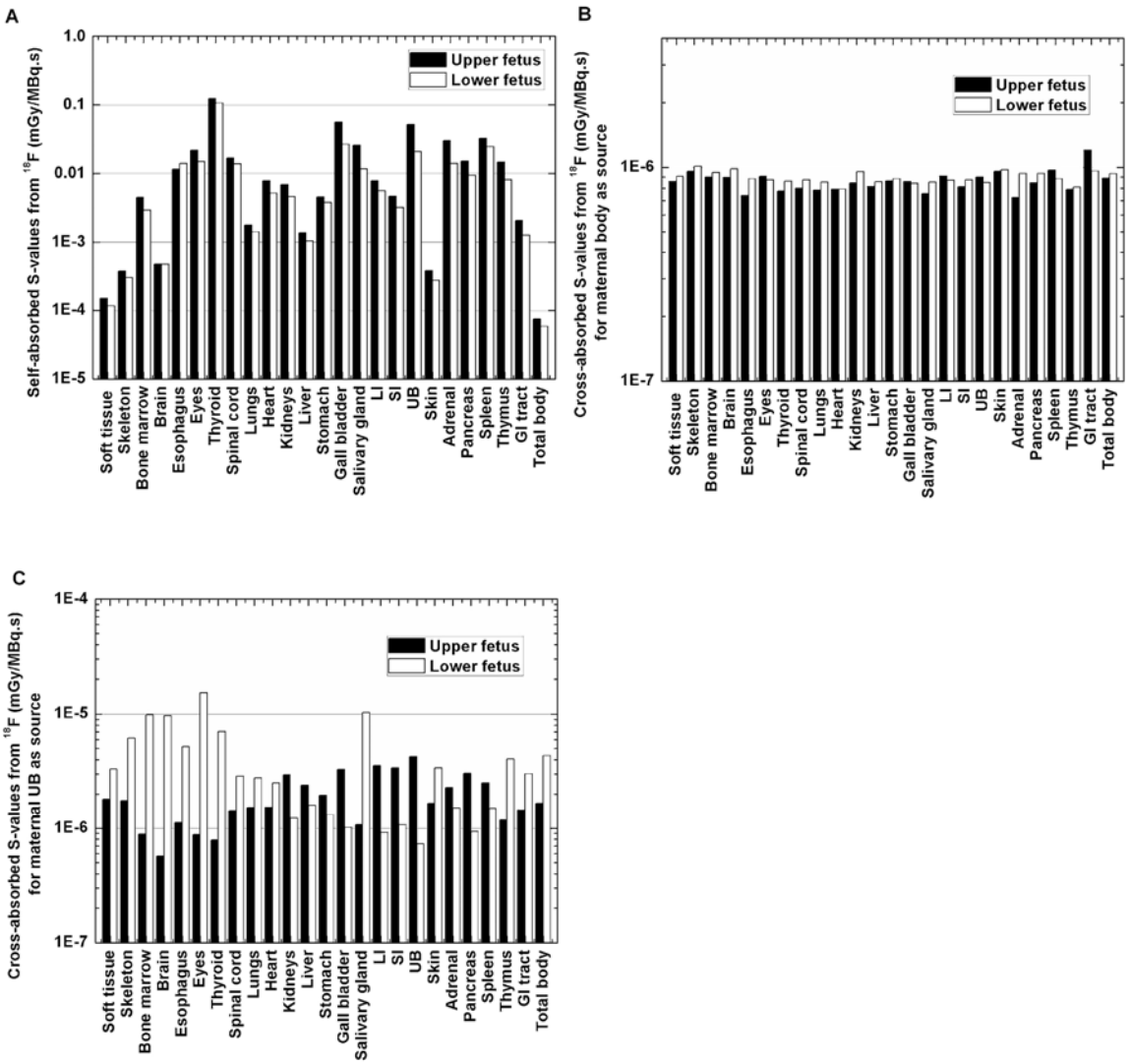

Fig. 4. (A) Self-absorbed S-values of F-18 for the fetal organs and cross-absorbed S-values of F-18 from (B) maternal body and (C) maternal UB, irradiating the fetal bodies (GI refers to gastrointestinal).

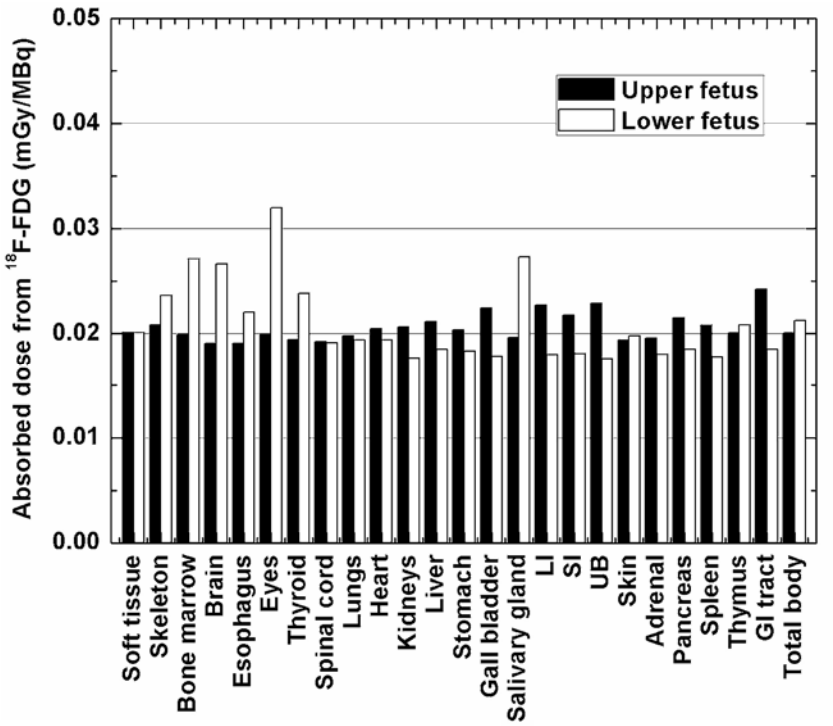

Fig. 5. Absorbed doses to different organs of the fetuses from ^{18}F-FDG.

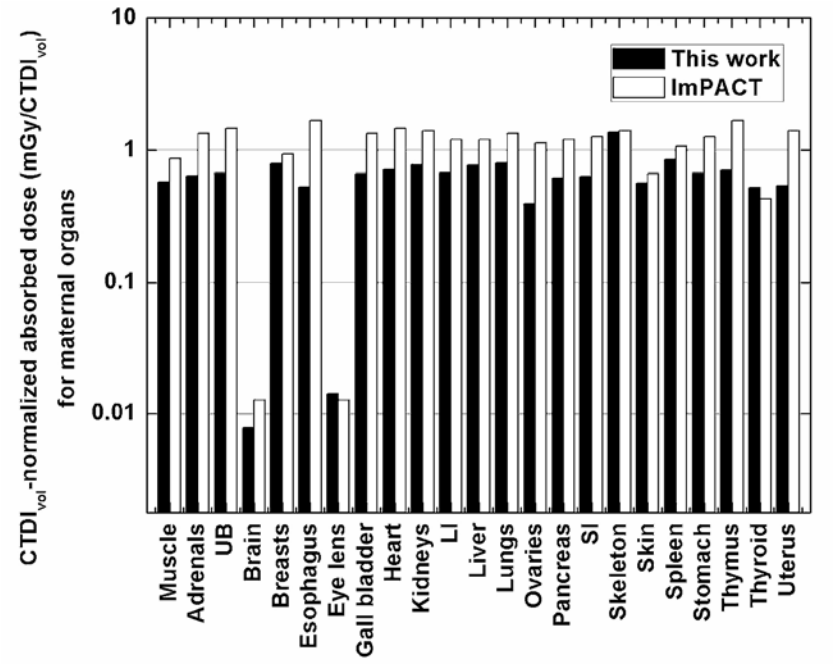

Fig. 6. Normalized absorbed doses to different organs of the pregnant patient from the CT examination.

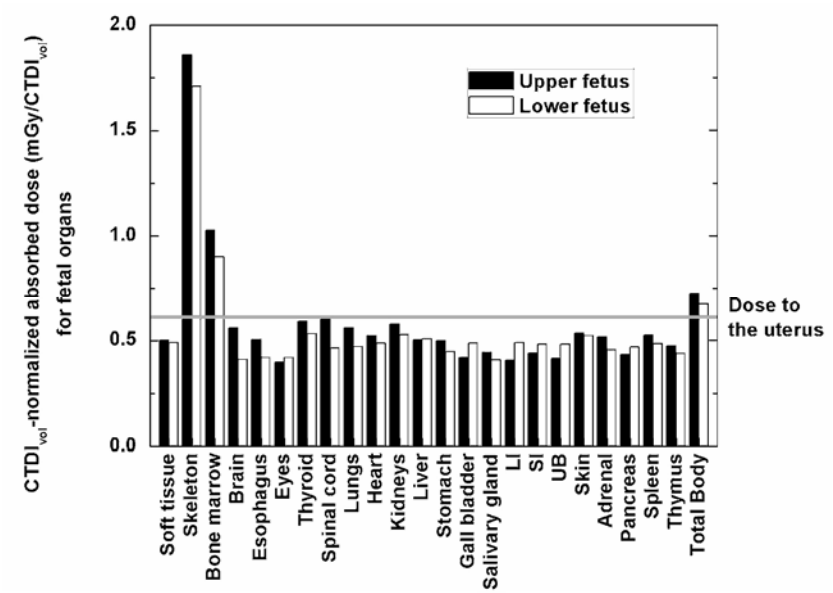

Fig. 7. Normalized absorbed doses to different organs of the fetuses from the CT examination.

Table 1. Total number of disintegrations of ^{18}F-FDG in maternal organs and fetuses.

Organ	Total number of disintegrations (Bq h/Bq)
Brain	0.21
Heart wall	0.11
Lungs	0.079
Liver	0.13
Bladder	0.3
Rest of the maternal body	1.7
Upper fetus	0.0412
Lower fetus	0.0434

Table 2. Organ masses of the fetus and lower fetuses.

Organs	Organ mass (g)	
	Upper fetus	Lower fetus
Soft tissue	326.3	425.1
Skeleton	117.3	148.4
Bone marrow	8.8	13.5
Brain	105.1	103.3
Esophagus	3.5	2.8
Eyes	1.9	2.7
Thyroid	0.3	0.4
Spinal cord	2.3	2.8
Lungs	24.8	31.0
Heart	5.4	8.3
Kidneys	6.0	9.0
Liver	33.0	44.3
Stomach	9.5	11.3
Gall bladder	0.7	1.5
Salivary gland	1.5	3.4
LI	5.2	7.3
SI	8.9	13.0
UB	0.8	2.0
Skin	104.9	147.4
Adrenal	1.3	2.9
Pancreas	2.7	4.5
Spleen	1.2	1.6
Thymus	2.8	5.1
Total body	774.3	991.7

Table 3. The total body doses from ^{18}F-FDG to the two fetuses compared with those obtained using OLINDA/EXM 1.1 and OLINDA/EXM 2.0.

Fetuses	Absorbed dose (mGy/MBq) from ^{18}F-FDG			Relative differences	
	OLINDA/EXM 1.1	OLINDA/EXM 2.0	This work	OLINDA/EXM 1.1 vs. This work	OLINDA/EXM 2.0 vs. This work
Upper fetus	0.00914	0.0121	0.0201	-54.50%	-39.76%
Lower fetus	0.00946	0.0125	0.0212	-55.45%	-41.13%

Table 4. Absorbed doses (mGy) and effective dose (mSv) to the maternal body from the PET/CT examination.

Maternal organs	Absorbed dose (mGy)		
	CT component	PET component	Total
Remainder	0.60	2.31	2.91
Adrenals	0.67	2.96	3.62
UB	0.70	13.02	13.72
Brain	0.01	7.77	7.78
Breasts	0.82	2.01	2.84
Esophagus	0.55	3.06	3.61
Eye lens	0.01	2.13	2.14
Gall bladder	0.69	3.34	4.03
Heart wall	0.74	16.35	17.08
Kidneys	0.81	2.76	3.57
LI wall	0.71	2.88	3.59
Liver	0.80	5.22	6.02
Lungs	0.84	3.93	4.76
Ovaries	0.41	3.22	3.63
Pancreas	0.64	2.99	3.63
SI	0.66	2.86	3.52
Skeleton	1.41	2.48	3.89
Skin	0.59	1.70	2.28
Spleen	0.88	2.65	3.53
Stomach	0.70	3.14	3.85
Thymus	0.73	3.97	4.71
Thyroid	0.55	2.20	2.75
Uterus	0.57	3.35	3.91
Total body	0.72	2.83	3.55
Effective dose (mSv)	0.79	3.62	4.41

Table 5. Absorbed doses to the fetuses from the PET/CT examination.

Fetal organs	Absorbed dose (mGy)					
	CT component		PET component		Total	
	Upper fetus	Lower fetus	Upper fetus	Lower fetus	Upper fetus	Lower fetus
Soft tissue	0.52	0.51	3.79	3.78	4.31	4.29
Skeleton	1.94	1.78	3.92	4.45	5.86	6.23
Bone marrow	1.07	0.94	3.75	5.10	4.81	6.04
Brain	0.58	0.43	3.59	5.01	4.17	5.44
Esophagus	0.53	0.44	3.58	4.14	4.11	4.58
Eyes	0.41	0.44	3.75	6.02	4.17	6.46
Thyroid	0.62	0.55	3.66	4.48	4.27	5.03
Spinal cord	0.64	0.48	3.62	3.59	4.26	4.08
Lungs	0.58	0.49	3.72	3.64	4.30	4.14
Heart	0.54	0.51	3.85	3.64	4.39	4.15
Kidneys	0.60	0.55	3.88	3.32	4.48	3.87
Liver	0.53	0.53	3.98	3.48	4.51	4.01
Stomach	0.52	0.47	3.83	3.45	4.35	3.92
Gall bladder	0.44	0.51	4.22	3.35	4.66	3.86
Salivary gland	0.46	0.43	3.69	5.14	4.15	5.56
LI	0.42	0.51	4.27	3.39	4.70	3.90
SI	0.46	0.50	4.09	3.40	4.55	3.90
UB	0.43	0.50	4.30	3.31	4.73	3.81
Skin	0.56	0.54	3.65	3.72	4.21	4.27
Adrenal	0.54	0.48	3.68	3.39	4.22	3.87
Pancreas	0.45	0.49	4.05	3.48	4.50	3.97
Spleen	0.55	0.51	3.91	3.34	4.46	3.85
Thymus	0.49	0.46	3.77	3.92	4.27	4.37
Total body	0.76	0.70	3.78	3.99	4.53	4.69